

## Research on the key technology of 8000mm diameter marine tracking dome

Libao Yang<sup>1, 2, a</sup>, Yanhong Li<sup>1</sup>, Jing Wang<sup>2</sup>, Yan Wang<sup>2</sup>, and Guoquan Shi<sup>1</sup>

<sup>1</sup> Changchun University of Science and Technology, Changchun 130033, China

<sup>2</sup> Changchun Institute of Optics, Fine mechanics and Physics, Chinese Academy of Sciences, Changchun 130033, China

<sup>a</sup>yanglibao228@163.com

**Keywords:** shipboard; marine environment; electro-optical tracking system; tracking dome; maximum tracking speed

**Abstract.** The shipboard electro-optical tracking system is facing the severe ocean climate environment. So it is necessary to consider the design of the carrier-based optoelectronic tracking system to prevent corrosion, moisture, mildew and salt fog. In addition to the passive protection of the photoelectric tracking system, the more effective way is to build the follow-up dome, to create a relatively good environment for the photoelectric tracking system, to achieve the purpose of active protection. But for the diameter of 8000mm with the development of super ship dome is still some key technology research. This paper makes a systematic research on the following aspects, such as the structure of the marine and the dynamic dome, the structural form of the bearing, the stiffness of the bearing, the analysis of wind resistance capacity and the azimuth drive system, and gives the corresponding research results. For the first time in China has been developed with the dome ship 8000mm in diameter, the maximum tracking speed is 22 DEG /s. Under the premise of ensuring the normal operation of the photoelectric tracking system, the purpose of protection is better.

### Overview

The shipboard electro-optical tracking system is facing the adverse ocean environment. Some factors such as high temperature, high humidity, corrosive substances, salt mist, mould and biological factors derived from them do great damage to the shipboard electro-optical system. It will absorb a layer of water film on the surface of the equipment in the humid marine atmosphere. It is the water film that form electrolyte membrane riching in salting, which is necessary for chemical corrosion and has strong corrosiveness on exposed metal surface<sup>[1, 2]</sup>. Besides, it will do irreparable harm on optical lens coating. So it is necessary to consider the design of the carrier based optoelectronic tracking system to prevent corrosion, moisture, mildew and salt fog.

In addition to the passive protection of the photoelectric tracking system, the more effective way is to build the follow-up dome, to achieve the purpose of active protection via creating a relatively good environment for the photoelectric tracking system. We can do it on the basis of studying previous shipboard domes.

There are several methods of opening the dome, including open the dome all used in LAMOST Telescope<sup>[3]</sup>. and tracking dome used in subgrade and shipboard<sup>[4-11]</sup>.

However there are still some key technologies to research for the development of the super ship dome with diameter of 8000mm. This paper makes a systematic research on the following aspects, such as the structure of the marine tracking dome, the structure of the bearing, the stiffness of the dome, the analysis of wind resistance capacity and the azimuth drive system, and gives the corresponding research results. The dome ship with 8000mm in diameter has been developed for the first time in China.

### Outline dimension of the dome and sphere structure

Fig. 1 shows the dome with 8000mm in diameter, it consists of transition connection, single row four point contact ball bearing, the upper part of the chassis, vault, skylight system, azimuth drive system, etc.

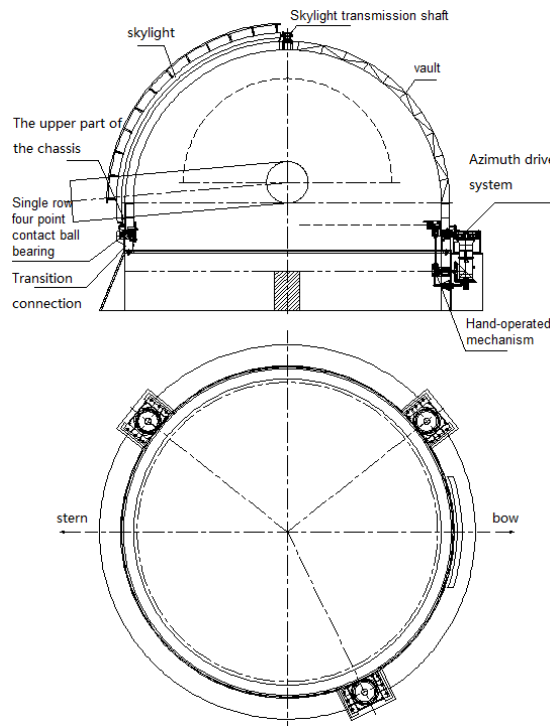


Fig. 1. Schematic diagram of Shipboard 8000mm dome.

**Transition connection.** Fig. 2 shows the transition connection which is important in connecting V bearing and the dome base.

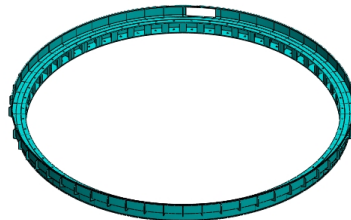


Fig. 2. Transition connection

**Single row four point contact ball bearing.** Fig. 3 shows the single row four point contact ball bearing, whose size is  $\phi 7966 \times 7380 \times 195$ , and having 0.1mm to 0.4mm in both radial clearance and axial clearance. Its end runout is  $\leq 0.4$ mm.

The bearing uses 42CrMo in both inner ring and outer ring, and the steel ball having 50.8mm in diameter uses GCr15. The bearing weights 11000kg in all.

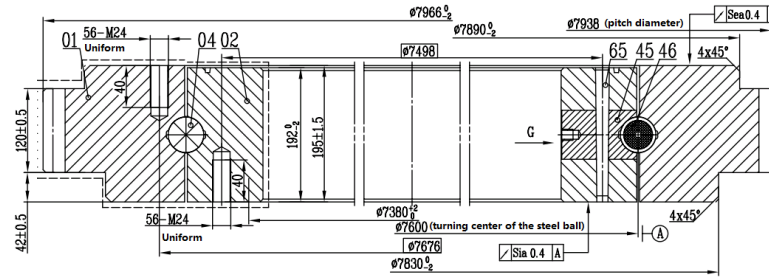


Fig.3. Single row four point contact ball bearing

**The upper part of the chassis.** Fig. 4 shows the upper part of the chassis, which is important in connecting the bearing moving coil and the vault.

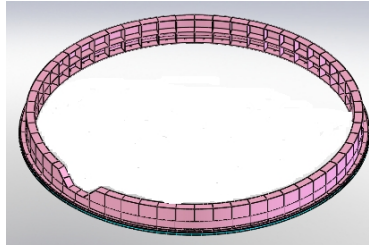


Fig.4. The upper part of the chassis

**Vault.** The vault is composed of frame which is made up of beam and arch and envelope.

Fig. 5(a) shows the structure of beam. There are 46 beams placed equally in 56 parts on the upper part of the chassis.

Fig. 5(b) illustrates the double-layer gird shape structure of the arch.

A hemisphere was combined after beams were assembled by mould into local spherical shells and then were welded with arch. A centring mandrel was assembled on the outside of the dome vertical center for fixing skylight center.

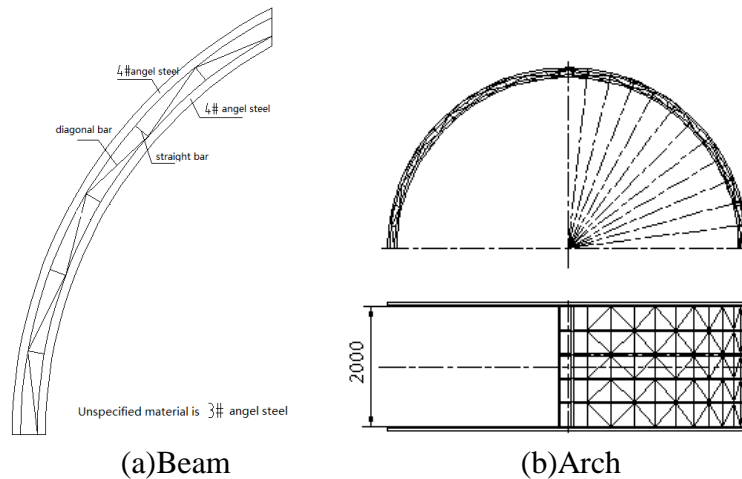


Fig.5

Owens Corning extruded foam thermal board FM250 insulation material is inside vault frame. The hemisphere weights 3200kg in all.

**Skylight system.** A skylight is put outside the vault, and be closing when the electro-optical tracking system is free and opening when the system is working, so that the dome could track to observe.

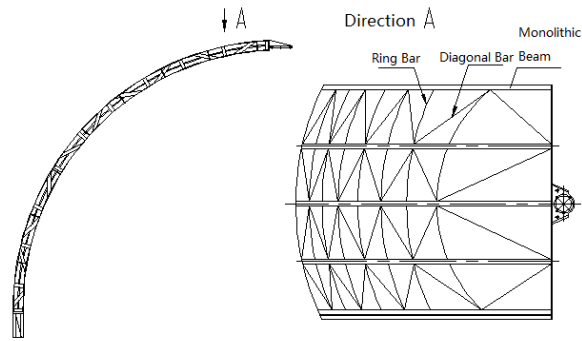


Fig.6 Skylight system

**Azimuth drive system.** The marine three-phase asynchronous motor drives the azimuth drive system of the dome. There is a absolute encoder on the dome.

The dome is driven by gear meshing. The outer ring of single row of four-point contact ball bearing is a large gear, bearing inner ring connected with the foundation, bearing outer ring connected with the dome, through the motor drive reducer on the pinion, driven by large gear rotation, to achieve dome rotation, as shown in Figure 7.

The dome is equipped with an absolute encoder, as shown in Figure 8. The absolute encoder is connected to the pinion on the gearbox through a first stage gear to achieve simultaneous rotation with the dome.

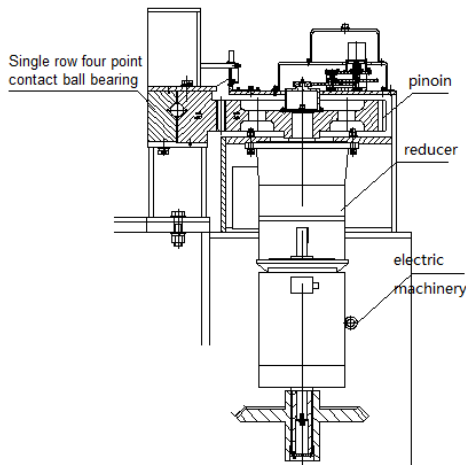


Fig. 7. Azimuth drive system

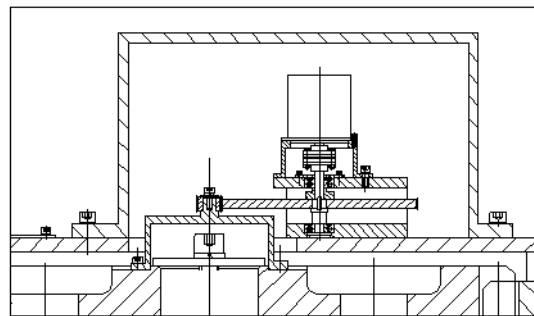


Fig. 8. Encoder system diagram

**Analysis and calculation of dome stiffness**

Jianghai Xu et al. proposed the applicable conditions and unfavorable factors of different astronomical dome according to the analysis results, which provided reference for the design of dome structure [12]. We calculated the wind load of the dome in the case of wind speed is 36.9m / s, while the ship navigating at 20.7m/s speed.

According to the wind pressure formula:

$$w_1 = \frac{1}{2} \rho v^2 \tag{1}$$

Where:

- $w_1$  --- wind pressure (N / m<sup>2</sup>)
- $\rho$  ---Air density at wind speed (1.293kg/m<sup>3</sup>)
- $v$  ---Wind speed (36.9m/s)

Calculation results:

Wind pressure at 36.9 m / s wind speed:  $\omega_1 = 880 \text{ N/m}^2$

Wind pressure at 20.7 m / s wind speed:  $\omega_2 = 277 \text{ N/m}^2$

Wind pressure in sum:  $\omega_0 = \omega_1 + \omega_2 = 1157 \text{ N/m}^2$

Taking into account the actual building height and building size of the case, the actual ball wind load is calculated by the following formula:

$$W_k = \mu_s \mu_z W_0 \quad (2)$$

Where:

$\omega_k$  --- Wind load standard value ( $\text{kg/m}^2$ )

$\mu_s$  --- Wind load shape coefficient

$\mu_z$  --- Height variation coefficient of wind pressure

$\omega_0$  --- Basic wind pressure ( $\text{N/m}^2$ )

According to the actual situation of installation and dome shape, we checked the "building structure commonly used data sheet" form. According to Table 1.3-43 wind load shape coefficient table,  $\mu_s = 0.6$ , while  $\mu_z = 1.14$  according to Table 1.3-42 wind pressure height variation coefficient table;

Wind pressure on the ball:  $\omega_k = 0.6 \times 1.14 \times 1157 = 791 \text{ N/m}^2$

Wind force on the ball side:

$$F = P \times \omega_k \times k = 791 \text{ N/m}^2 \times 28 \text{ m}^2 \times 0.4 = 8859 \text{ N} \quad (3)$$

Where:

A --- Wind cross section area (calculate in case of hemisphere having 7780mm in diameter)

$\omega_k$  --- The wind pressure of the sphere

k --- The wind force coefficient of the ball is 0.4

**Displacement and Stress Analysis of Arch Beam.** According to the analysis, the force of the monolithic arch beam is about 2953N by one third force. Then we did finite element analysis of monolithic arch girder, Fig. 9 is the displacement analysis diagram of monolithic arch beam; Fig.10 shows the stress analysis of monolithic arch beam.

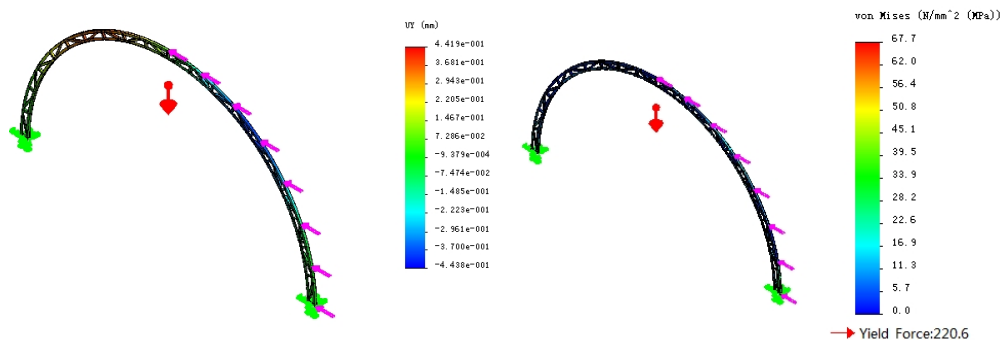


Fig.9. Single arch displacement analysis chart Fig.10. Stress analysis of monolithic arch

According to the analysis results in Fig. 9, the maximum displacement of the monolithic arch beam is 0.44mm, which is within the allowable displacement range of the elastic deformation. According to the analysis results in Fig. 10, the maximum stress of the monolithic arch beam is 67.7MPa, less than allowable stress 220.6MPa.

**Displacement and Stress Analysis of Beam.** The displacement of the beam only caused by its own gravity is shown in Fig11.

According to the analysis results, the maximum displacement above the beam is  $1.5 \times 10^{-4}$  mm, within the allowable range of elastic deformation.

The wind force on the side of the sphere is also 8859N when the stress of the single piece beam is analyzed, this force is distributed to the beam, and the force is about 2953N by  $60^\circ$  on two pieces and  $90^\circ$  on one piece, Fig. 12 shows the stress analysis of the beam.

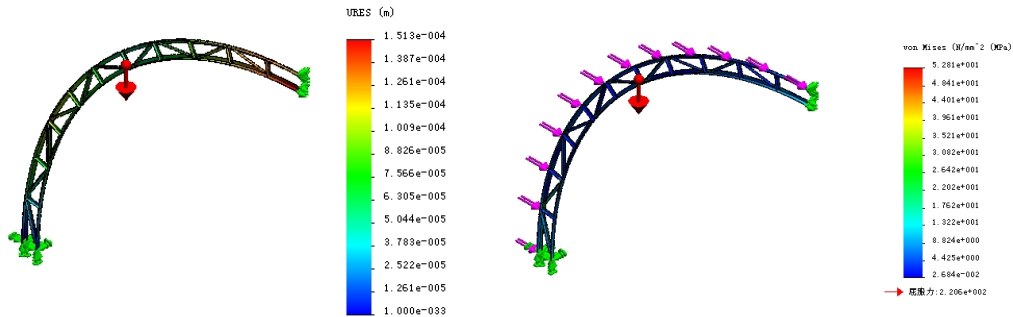


Fig. 11. Deformation displacement of beam Fig. 12. Analysis of stress plate girder

It can be seen from Fig. 12 that the maximum stress of the beam is 52.81MPa, less than the allowable stress 220.6MPa.

**Calculation of Dome azimuth drive**

**Calculation of Moment of Inertia.** It is required that dome rotating speed should not be less than  $22^\circ / s$ , while acceleration is  $7^\circ / s^2$ , so the speed of gear is  $3.67r / min$ .

**Calculation of the moment of inertia of the ball steel frame.** The dome ball steel frame is simplified to a thin spherical shell modeling that be equal weight and equal outer diameter to the dome, calculated by software, as shown in Figure 13.

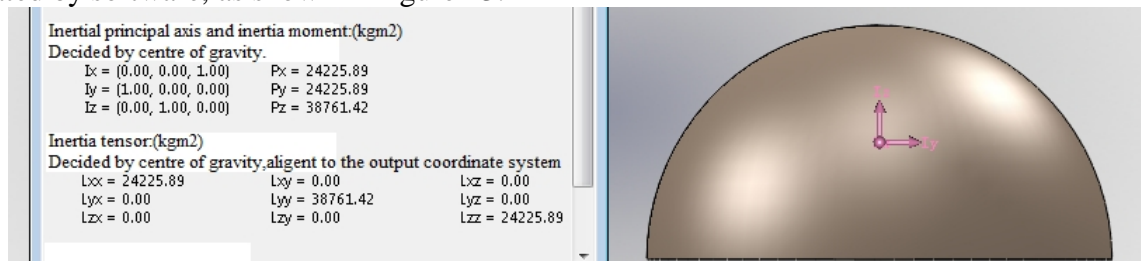


Figure 13 simulation of steel sphere of inertia

The result calculated by software is  $J_1 = 38761 \text{ kgm}^2$ .

**Calculation of the moment of inertia of the inside and outside the mask.** It is calculated by software, as shown in Fig.14.

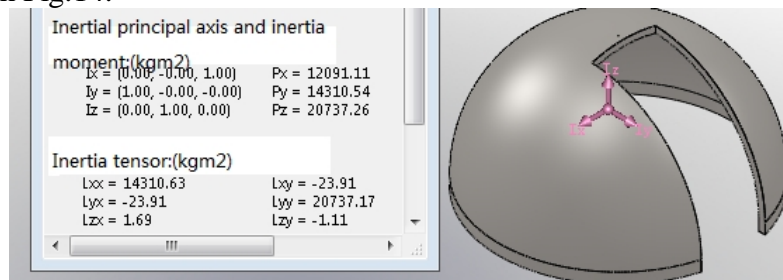


Fig.14. Inside and outside the mask of inertia

The result calculated by software is  $J_2 = 20737 \text{ kgm}^2$ .

**Calculation of the moment of inertia of the ball steel frame.** The inertia of the upper chassis is calculated by software, as shown in Figure 15.

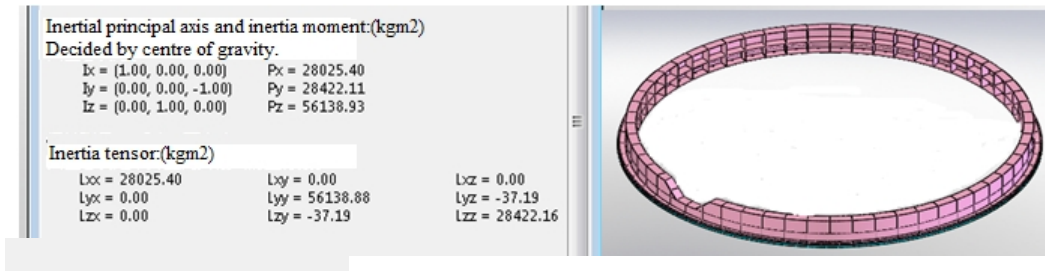


Fig. 15. Inertia of the upper chassis

The result calculated by software is  $J_3 = 56139 \text{ kgm}^2$ .

**Calculation of the moment of inertia of the ball steel frame.** Figure 16 shows the moment of inertia of drive rotary bearing ring of the dome calculated by software.

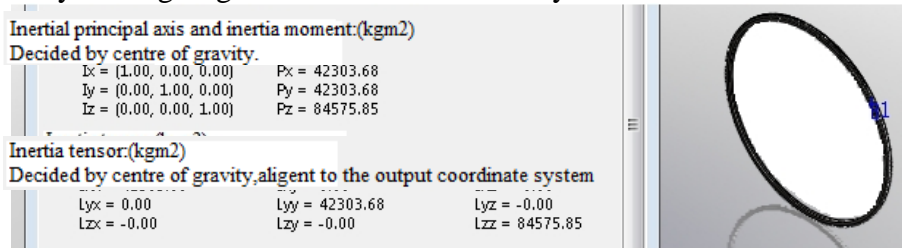


Fig. 16. moment of inertia of the outer rotating ring of the bearing

The result calculated by software is  $J_4 = 84576 \text{ kgm}^2$ .

So the moment of inertia of the dome in sum is  $J = J_1 + J_2 + J_3 + J_4 = 200213 \text{ kgm}^2$ .

**Motor and reducer selection.** In the normal work, the lateral force also produces a certain torque on the dome. Assume that the dome is under the fresh gale while the vessel is sailing at a speed of 20.7 m / s.

The wind speed of the fresh gale is  $v = 20.7 \text{ m / s}$ , while the wind pressure per unit area is  $P_1 = 26.78 \text{ kg / m}^2$ , and the wind pressure caused by the hull velocity is  $P_2 = 26.78 \text{ kg / m}^2$ , so the total wind pressure is  $P = P_1 + P_2 = 53.56 \text{ kg / m}^2$ ;

The side area of the skylight is  $S = 1.2 \text{ m}^2$ ;

The wind power on the side area of the skylight is 630 N, and the force radius is 3.4 m, so the torque produced by the lateral force on the dome is  $T' = 630 \times 3.4 = 2142 \text{ Nm}$ .

Basing on the total moment of inertia of the dome is known, so the maximum torque required on the large ring gear is:

$$T_2 = J \times \alpha + T' = 200213 \times 0.1222 + 2142 = 26608 \text{ Nm.} \tag{4}$$

Where:

$T_2$  ——The torque required on the large ring gear;

$J$  ——The total moment of inertia of the dome;

$\alpha$  ——The angular acceleration of the dome rotation(Calculated at  $7^\circ / \text{s}^2$  acceleration).

We choose primary gear reducer ratio of 1:23, and motor speed of 1460r / min, then the size of the gear ratio should be about  $i = 12.886$ .

So the torque of the torque is  $T_1 = T_2 / 12.886 / 0.94 = 2197 \text{ Nm}$  (0.94 for gear transmission efficiency).

Motor Power is  $P = T_2 \times n / 9550 = 26608 \times 3.667 / 9550 = 10.2 \text{ kw}$ .

$P_{\text{electric machinery}} = P / \eta_{\text{bearing}} / \eta_{\text{reducer}} = 10.2 / 0.94 / 0.94 = 11.34 \text{ kw}$ .

According to the above data we made selection of three XWD7 cycloid reducer, with reduction ratio of 1:23, and three Y2-160L-4 1460r / min 15kw three-phase asynchronous motor, so that a single

reducer rated output torque is 1450Nm, and the sum of three reducers is 4350 Nm, which is twice the value of T1 (2197Nm) and can meet the maximum acceleration requirements of  $7^\circ / s^2$ .

We calculated the maximum speed  $n = 1460/23 / 12.88 = 4.928 \text{ r / min} = 29.5^\circ / s$ , basing on motor speed is 1460 r / min, speed ratio on reducer is 1:23, and the gear ratio is 1: 12.886, meeting the Speed requirements for  $22^\circ / s$ .

The installation process of marine follow-up dome is shown in Figure 17.

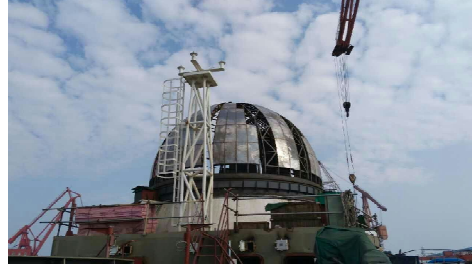


Fig. 17. the construction process of the moving dome

## Conclusions

In order to adapt the shipboard photoelectric tracking system to the harsh marine environment, the researchers are very concerned about the protection technology research. The installation of the follow-up dome is a good choice, it is hoped that it can achieve the protection of the optical tracking system while does not affect the normal tracking system. This paper studies the strength analysis and maximum tracking speed et al. of the moving dome. Through simulation analysis and practice verification, a series of research results are obtained. We successfully developed a marine tracking dome with diameter of  $\phi 8000\text{mm}$  and the maximum tracking speed of  $22^\circ / s$ . We achieved the purpose of a better protection while ensuring the normal operation of the photoelectric tracking system.

## References

- [1] Weiguo ZHANG, Yukun WANG, Bin WANG, Da YANG. Design and three-proofing technique of shipboard optic-electronic equipment [J]. *INFRARED TECHNOLOGY*. 2008, 30 (4):214-216. (In Chinese)
- [2] Youheng MA, Peiguo LU, Yulin GUO et al. Environmental worthiness design of shipboard electro-optical system[J].*JOURNAL OF APPLIED OPTICS*, 2014,35(3) :371-376. (In Chinese)
- [3] Yongheng Zhao. Spectroscopic surveys of LAMOST [J]. *Physics*. 2015, 44(4):205-212. (In Chinese)
- [4] Bei ZHANG, Huibin GAO. Active disturbance rejection control algorithm research for large tracking dome system[J].*Science Technology and Engineering*. 2016, 16(26):75-79. (In Chinese)
- [5] Changyou LIU. Tracking dome on the trailer [J].*Opt. Precision Eng.* 1995, 3(5):121-125. (In Chinese).
- [6] *OME Information*. 2011 , 28 (9):18-28. (In Chinese)
- [7] Jingxu ZHANG. Structure types and design principles of ground-based telescope enclosures[J]. *Chinese Optics*. 2012, 5(2):126-132. (In Chinese)
- [8] Tongsheng MAO, Sheyang JIANG. The dome of the 2.16 meter reflecting telescope [J].*ACTA ASTRONOMICA SINICA*,1992,33(2):220-228 (In Chinese)



- [9] Qinchang LIN, Yuan LIN, Jianhua ZHANG. A new method for follower to control the telescope domes [J]. Annual of Shanghai Observatory of Chinese Academy Sciences, 2001, 22:122-126. (In Chinese)
- [10] Zhengqiu YAO, Fang ZHOU. Progress in modern astronomical enclosure [J] . Progress in Astronomy. 2003, 21(3):206-218. (In Chinese)
- [11] CHENG Ying-wei. Achieving dome slit driving and status detection with two conductive rings [J]. Astronomical Research and Technology. 2016, 13(2): 213-218. (In Chinese)
- [12] Jianghai XU, Xuefei GONG. Study of wind load on four astronomical enclosures based on numerical wind tunnel experiments [J]. ACTA OPTICA SINICA. 2015, 35(5):0501005-1-0501005-15. (In Chinese)